



Bacterial cellulose-based indicators for freshness monitoring in intelligent packaging of fresh-cut jackfruit

Nurul Iswati¹, Andi Dirpan^{1,2*}, Adiansyah Syarifuddin¹, Serli Hatul Hidayat^{1,2}, Andi Fadiah Ainani^{1,2}, and Soumya Majumder^{2,3}

¹ Faculty of Agricultural Technology, Hasanuddin University, Makassar 90245, Indonesia

² Research Group for Post-Harvest Technology and Biotechnology, Makassar 90245, Indonesia

³ Department of Tea Science, University of North Bengal, Darjeeling 734013, India

Abstract

Fresh-cut fruits are highly perishable due to rapid physiological, chemical, and microbiological changes during storage, which limit their shelf life and consumer acceptance. To address this challenge, this study developed bacterial cellulose-based indicator labels combined with colorimetric solutions to provide real-time information on the quality of fresh-cut jackfruit as part of intelligent packaging. This study focused on identifying the most suitable color indicator for jackfruit and evaluating the performance of the bacterial cellulose-based label in detecting freshness. Indicators were tested during 24 hours of storage at room temperature, and their responses were correlated with key quality parameters, including O₂ and CO₂ concentrations, firmness, pH, total soluble solids, vitamin C, total acidity, and microbial counts. The results demonstrated that the developed indicator effectively responded to quality changes, with color shifts reflecting respiration activity, tissue softening, biochemical alterations, and microbial growth. Correlation analysis confirmed that the indicator's color changes were consistent with the deterioration of fresh-cut jackfruit, particularly after 20 hours when microbial counts exceeded acceptable limits. Overall, intelligent packaging based on bacterial cellulose indicators offers an accurate, consumer-safe, and sustainable solution for monitoring fruit freshness.

Article History

Received September 8, 2023

Accepted December 19, 2025

Published December 31, 2025

Keywords

Fresh-cut
Jackfruit,
Intelligent Packaging,
Bacterial Cellulose

1. Introduction

Global socioeconomic development has contributed to substantial shifts in dietary patterns across many populations. Modern consumers increasingly prefer practical, nutrient-dense foods, including fresh-cut fruits and vegetables. The growing consumption of fresh-cut products is driven by heightened health awareness and global initiatives that encourage greater intake of fruits and vegetables as part of a balanced diet (1,2). This trend is reflected in the growing awareness of the role of plant-based nutrition in maintaining health and preventing diseases followed by increasing availability and consumption of fresh-cut fruits and vegetables, which are perceived as convenient and beneficial to health (3–5). In addition, the fast-paced nature of urban lifestyles encourages consumers to choose practical foods without compromising nutritional value, making fresh-cut fruits a preferred option due to their ready-to-eat characteristics (2). Such developments indicate a broader shift toward dietary patterns that rely more heavily on fresh fruit and vegetable consumption (6).

* Correspondence : Andi Dirpan

 dirpan@unhas.ac.id

However, despite their increasing popularity, fresh-cut fruits are highly susceptible to quality deterioration caused by mechanical damage, enzymatic reactions, microbial growth, and oxidative processes triggered by minimal processing and postharvest handling (7,8).

Intelligent packaging has emerged as a critical innovation for monitoring and preserving the quality of fresh fruits. This technology relies on chemical indicators capable of detecting changes in food composition, such as reactions with microbial metabolites or color shifts triggered by variations in pH, temperature, or spoilage-related compounds (9,10). These indicators provide clear visual cues that enable real-time quality assessment, allowing consumers to directly evaluate fruit freshness and enhancing transparency throughout the supply chain (11). By offering early warnings of quality deterioration, intelligent packaging helps reduce spoilage at the consumer level and encourages timely consumption rather than disposal (10,12). Moreover, this technology plays a significant role in mitigating food loss and food waste, a critical global challenge, by improving the accuracy of quality monitoring so that fewer overripe or damaged products reach retailers, and consumers are less likely to discard fruits prematurely (13–15).

One form of intelligent packaging currently being developed is smart packaging based on bacterial cellulose (BC). The main advantage of BC as a biodegradable film material lies in its higher purity compared to plant cellulose, as it is free from hemicellulose, lignin, and other non-cellulosic compounds (16). BC also demonstrates excellent liquid absorption capacity, high polymerization strength, and a much greater degree of crystallinity than plant cellulose, resulting in superior mechanical properties. In addition, BC possesses high tensile strength and a highly porous nanofibril structure, which facilitates efficient loading of indicators, strengthens interactions with spoilage compounds, and accelerates responses to changes in pH and metabolic gases (12,17). Furthermore, bacterial cellulose (BC) demonstrates excellent biocompatibility, environmental sustainability, and complete biodegradability (18).

Research on cellulose-based intelligent packaging has been applied to meat (19–22), chicken (23–26), fish (27–30), vegetables (17,31,32) and non-tropical fruits such as strawberry (33), apple (34) and pear (35). However, the application to tropical fruits, particularly fresh-cut jackfruit, has not been explored. Therefore, this study aims to develop and characterize a cellulose-based indicator label combined with a color indicator solution. This study also focuses on determining the most appropriate type of color indicator to use on jackfruit, as well as testing the performance of the bacterial cellulose-based indicator to assess its effectiveness in detecting fruit freshness. Overall, these findings confirm the potential of bacterial cellulose-based indicator labels, which provide a simple visual system for monitoring fruit freshness, ensuring product safety, and reducing food waste.

2. Materials and Methods

2.1. Preparation of Fresh-Cut Jackfruit

Jackfruit (*Artocarpus heterophyllus* Lam.) was purchased from a traditional market (Gowa). The jackfruit used was fully ripe, yellowish in color, emitting a characteristic aroma, and of medium size (± 6 kg, length 35–39 cm). After being obtained, the fruit underwent minimal processing, consisting of simple cutting and handling to obtain the edible portion in the form of arils or ripe bulbs.

2.2. Preparation of Intelligent Packaging Indicators

Color indicator solutions were prepared by dissolving the indicators at a concentration of 1% (v/v) in 50% ethanol (36). The indicators used were Methyl Red (MR) (Arkitos, Surabaya), Bromothymol Blue (BB) (Merck, Darmstadt, Germany, CAS No. 76-59-5), and Phenol Red (PR) (Merck, Darmstadt, Germany, CAS No. 34487-61-1). The pH of the solutions was then adjusted using NaOH and CH₃COOH. In this study, the pH values applied were: Methyl Red (pH 6.2), Bromothymol Blue (pH 7.6), and Phenol Red (pH 8.1).

2.3. Preparation of Bacterial Cellulose Film

Bacterial cellulose membranes were prepared using mature coconut water (11–12 months old) obtained from the traditional market of Antang, Makassar, which was left to stand for 5 days to reduce the pH. The coconut water was boiled and supplemented with 5% (w/v) sucrose, 1% (v/v) acetic acid (CH₃COOH), and 0.5% (w/v) nitrogen source (ZA Food Grade, Online Market). Subsequently, 1 L of hot coconut water was poured into a sterilized container, covered with sterile paper, and allowed to cool. After cooling, the medium was inoculated with 10% (v/v) *Acetobacter xylinum* starter (online market) and incubated for 7 days at 30 °C. Once the cellulose membrane was formed, purification was carried out by immersing the microbial cellulose in 5% (v/w) NaOH solution, covered with aluminum foil, for 24 hours. The cellulose was then repeatedly rinsed with distilled water until reaching a neutral pH of 7.0. Finally, the bacterial cellulose membrane was pressed flat using a hand press and dried in an oven at 110 °C for 2 hours.

2.4. Fabrication of Indicator Film Labels

The bacterial cellulose sheets obtained were first cut into dimensions of 3 × 4 cm, then immersed in the prepared color indicator solutions for 24 hours. Following immersion, the sheets were rinsed with running water to reduce excessive binding between the color solution and the cellulose membrane. Finally, the film was dried using an electric hair dryer (Philips). The complete procedure for the fabrication of bacterial cellulose–based indicator film labels is illustrated in Figure 1.

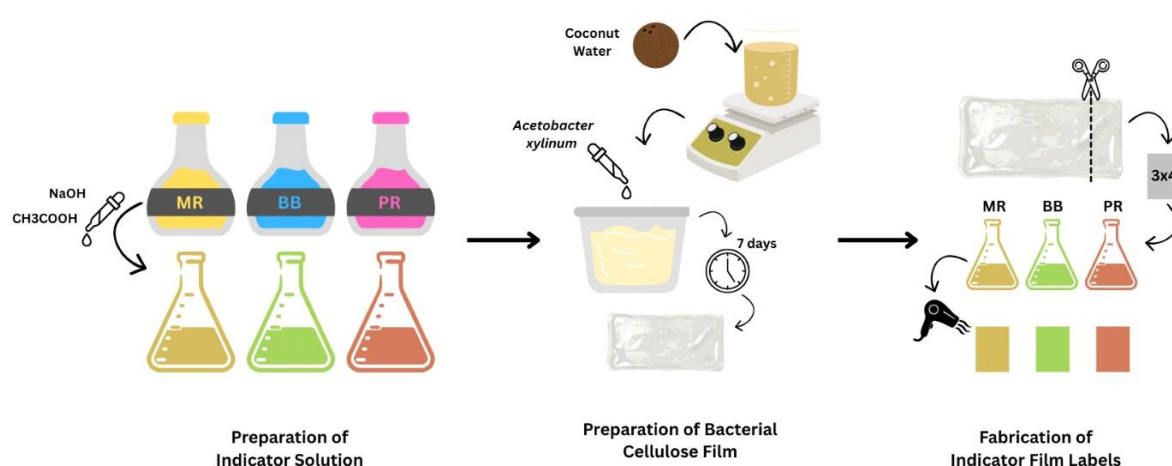


Figure 1. Preparation of the indicator solution and bacterial cellulose film for indicator labels [Methyl Red (MR), Bromothymol Blue (BB), and Phenol Red (PR)].

2.5. Application of Intelligent Packaging on Fresh-Cut Jackfruit

A total of 250 g of fresh-cut jackfruit was placed into a polypropylene (PP) container. The prepared indicator label was attached to the inner side of the container lid (Figure 2). The container was then sealed and stored at room temperature (25 ± 3 °C) for 24 h. Changes in the color of the indicator label and the freshness quality of the jackfruit were observed at 0, 4, 8, 12, 16, 20, and 24 h.

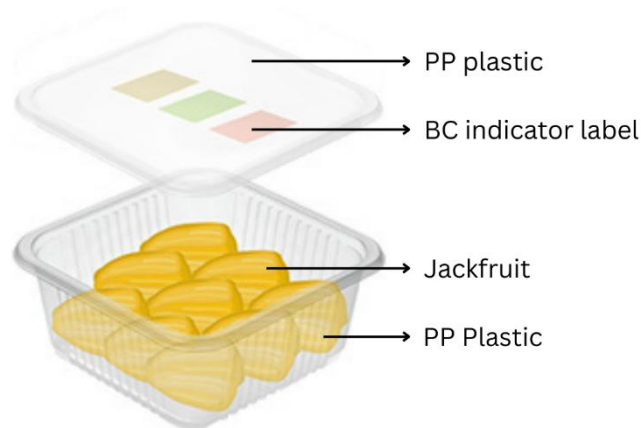


Figure 2. Application of bacterial cellulose film indicator on fresh-cut jackfruit.

2.6. Thickness Analysis of Bacterial Cellulose Indicator Labels

The thickness of the cellulose sheets was measured using a caliper from various sides and the formed labels.

2.7. Moisture Content Analysis of Bacterial Cellulose Indicator Labels

Cellulose 1 g was weighed and transferred into the moisture analyzer dish. The temperature of the instrument was set to 105 °C, the lid was closed, and the process was allowed to run until the moisture content was determined. The obtained value was then recorded.

2.8. Chemical Structure of the Bacterial Cellulose Indicator Label

The chemical structure of the freshness indicator label was determined using Fourier Transform Infrared (FTIR) spectroscopy (Shimadzu IRSpirit). FTIR analysis was conducted to identify the interactions among functional groups within the label structure. The measurements were performed at a resolution of 1 cm^{-1} , with average scanning in the range of $4000\text{--}500 \text{ cm}^{-1}$, and operated in Attenuated Total Reflection (ATR) mode.

2.9. Biodegradation Analysis of the Bacterial Cellulose Indicator Label

Biodegradation testing was carried out using the soil burial method with compost soil, where the samples were buried and left until complete decomposition occurred. The degradation process was observed at time intervals of 3, 6, 9, 12, and 15 days.

2.10. Color Analysis of the Bacterial Cellulose Indicator Label

The bacterial cellulose indicator labels were photographed using a digital camera (Sony A6000). The color change data were obtained in the form of L^* , a^* , and b^* values based on the Hunter's Lab Colorimetric System using a colorimeter (AMT 507), with the readings taken without opening the package lid. These values were then converted into °Hue and ΔE (9).

2.11. Chemical Analyses of Fresh-Cut Jackfruit

The analyses conducted on fresh-cut jackfruit included colorimetry with ΔE value calculation using a colorimeter (AMT 507), measurement of CO₂ and O₂ gases using a CO₂ analyzer (Sentry ST303), hardness testing with a penetrometer, pH measurement using Phs-3C, determination of total soluble solids with a digital refractometer, assessment of vitamin C content, analysis of total acidity, and Total Plate Count (TPC).

2.12. Statistical Analysis

Each experiment was performed in triplicate, and the resulting data were analyzed using analysis of variance (ANOVA) with SPSS version 25. Significant differences among means were further evaluated using Duncan's Multiple Range Test at a significance level of $p < 0.05$. All results are presented as mean values \pm standard deviation (SD).

3. Results and Discussion

3.1. Physical Properties of The Bacterial Cellulose Indicator Label

3.1.1. Thickness and Water Content





The thickness of bacterial cellulose, as shown in Table 1, exhibited a highly significant difference between the control sample and the treatments with indicator labels, which was closely related to the moisture content contained within them. The control sample demonstrated the greatest thickness (87.33 mm) and the highest moisture content (92.43%), whereas the three treatments with indicators (MR, BB, PR) showed extremely thin thicknesses (1.05 mm, 1.03 mm, and 1.13 mm) and much lower moisture contents (10.7%, 10.33%, and 9.93%). The cellulose produced by *Acetobacter xylinum* is a product of its metabolic process, in which the cellulose molecules formed are cross-linked, creating a nata layer that gradually accumulates and thickens (37). Higher moisture content tends to cause the film structure to swell and form thicker layers, while drying reduces the swelling ability of bacterial cellulose (38). Bacterial cellulose resembles a hydrogel membrane due to its fibrous, net-like structure, which enables it to retain large amounts of water (39). Pressing and drying treatments reduce the water content, resulting in thin polymeric film sheets. Pressing functions to decrease moisture and flatten the surface, while oven drying helps evaporate residual moisture and strengthen the film structure (40).

3.1.2. Colorimetric Properties

Color characteristics in the colorimetric analysis were evaluated using Lab and Hue parameters. The L value represents brightness, ranging from black (0) to white (100), while a* values indicates the color gradients from green to red while b* signifies blue to yellow (41). Colorimetric data in Table 1 show that the control sample exhibited moderate brightness ($L^* = 52.21$) with low negative a* and b* values (-0.68 ; -4.07), reflecting minimal color saturation and a neutral whitish appearance. Treatments with color indicators resulted in a marked decrease in brightness, as indicated by L^* values for MR (41.09), BB (37.08), and PR, which had the lowest value (34.95), along with significant visual differences in a* and b* parameters. Methyl Red (MR) produced an orange-reddish hue ($a^* = 12.52$; $b^* = 13.59$), Bromothymol Blue (BB) shifted toward a brownish-yellow hue ($a^* = 0.88$; $b^* = 7.46$), whereas Phenol Red (PR) showed a dominance of dark red ($a^* = 14.17$; $b^* = 4.00$). Hue analysis, as a parameter for identifying dominant color components in the light spectrum (42), reinforced these findings: PR exhibited the lowest Hue value (15.78°), indicating strong red dominance; MR was in the

intermediate range (47.37°), corresponding to orange due to the combination of red and yellow; while BB (83.2°) and the control (79.88°) tended toward bluish-green, although the control appeared more neutral due to its low saturation (43).

Table 1. Results of thickness, moisture content, and color analysis of bacterial cellulose in the control sample and indicator labels (MR, BB, and PR).

Parameters	Control	MR	BB	PR
Thickness (mm)	87.33 ± 2.52^b	1.05 ± 0.08^a	1.03 ± 0.15^a	1.13 ± 0.15^a
Moisture Content (%)	92.43 ± 2.5^b	10.7 ± 0.56^a	10.33 ± 0.91^a	9.93 ± 1.21^a
Color	L*	52.21 ± 3.08^c	41.09 ± 0.99^b	37.08 ± 1.86^{ab}
	a*	-0.68 ± 0.11^a	12.52 ± 0.73^d	0.88 ± 0.05^c
	b*	-4.07 ± 1.17^a	13.59 ± 0.17^c	7.46 ± 1.32^b
	°Hue	79.88 ± 4^c	47.37 ± 1.36^b	83.2 ± 0.87^c
Apparent color				

Note. Data are expressed as mean \pm standard deviation. Distinct letters within the same column denote significant differences ($p < 0.05$)

3.2. FTIR Analysis of the Bacterial Cellulose Indicator Label

The FTIR spectra of bacterial cellulose indicator labels containing Methyl Red, Bromothymol Blue, and Phenol Red are presented in Figure 3. The spectra reveal a narrow band at 3742 cm^{-1} and a broad band at 3344 cm^{-1} , corresponding to hydroxyl groups ($-\text{OH}$), both in free form (free OH) (44) and bound form (intra H-bond), which indicate the presence of α -cellulose (45,46). The band at 2893 cm^{-1} represents C–H stretching ($-\text{CH}$ and $-\text{CH}_2$ groups) of cellulose and hemicellulose components (47). A strong absorption band at 1642 cm^{-1} corresponds to carboxylic acid groups ($-\text{COOH}$) within the cellulose structure (48), consisting of carbon atoms bonded to carbonyl ($\text{C}=\text{O}$) groups (34) and hydroxyl ($-\text{OH}$) groups (49). The band at 1424 cm^{-1} indicates the presence of carbonyl ($\text{C}=\text{O}$) groups (48) or CH_2 stretching of carbon–hydrogen bonds in methylene groups ($-\text{CH}_2-$) (47). Meanwhile, the band at 1319 cm^{-1} can be attributed to C–H deformation (50) or CH_2 wagging (45). Finally, the band at 1022 cm^{-1} corresponds to C–O–C (ester) groups (45,48,51–53).

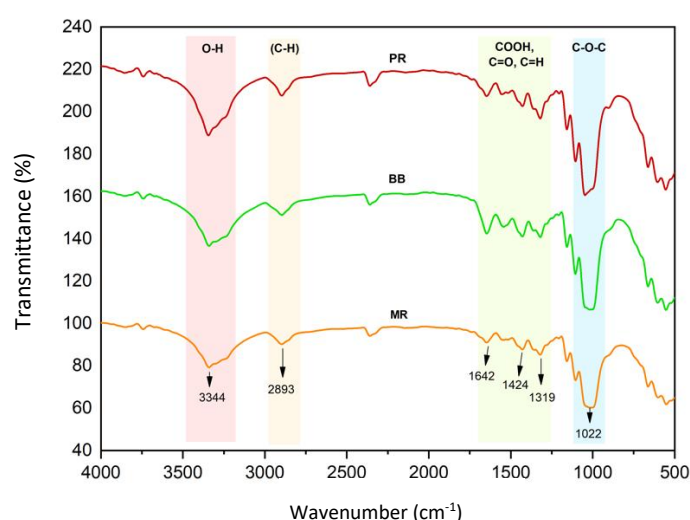


Figure 3. FTIR spectra of bacterial cellulose–based indicator labels incorporated with methyl red (MR), bromothymol blue (BB), and phenol red (PR).

3.3. Biodegradability of the Bacterial Cellulose Indicator Label

Biodegradation testing was conducted to determine the extent to which the indicator labels could be decomposed by soil microbial activity. The degradation patterns of bacterial cellulose-based indicator labels in Figure 4 and Table 2 containing Methyl Red (MR), Bromothymol Blue (BB), and Phenol Red (PR) were monitored over a storage period of 15 days. On day 3, slow degradation was observed with values of MR (9.41%), BB (16.19%), and PR (11.57%). By day 6, degradation increased in MR (17.45%) and BB (24.58%), while PR (10.12%) showed a decrease; however, the differences among treatments were not statistically significant. A sharp increase occurred on day 9, with MR (52.75%), BB (55.28%), and PR (74.06%), followed by consistently high degradation on day 12, where MR (55.29%), BB (53.23%), and PR (71.69%). By day 15, all treatments showed degradation values of 0.00%, which can be interpreted as the final stage of decomposition or cessation of microbial activity, indicating no further degradation.

Changes in the physical and mechanical properties of bacterial cellulose (BC) films occurred as a result of decomposition in soil. When BC films were directly composted, soil microorganisms broke down degradable components into carbon dioxide, methane, water, and biomass (54). This degradation process was primarily driven by microbial activity, with fungi such as *Aspergillus unguis* and *Paecilomyces marquandii* identified as effective agents in degrading bacterial cellulose through cellulase enzyme production (55). In addition, bacteria such as *Bacillus* sp. and *Rhizopus* sp. were also reported to contribute significantly to the breakdown of cellulose structures (56).

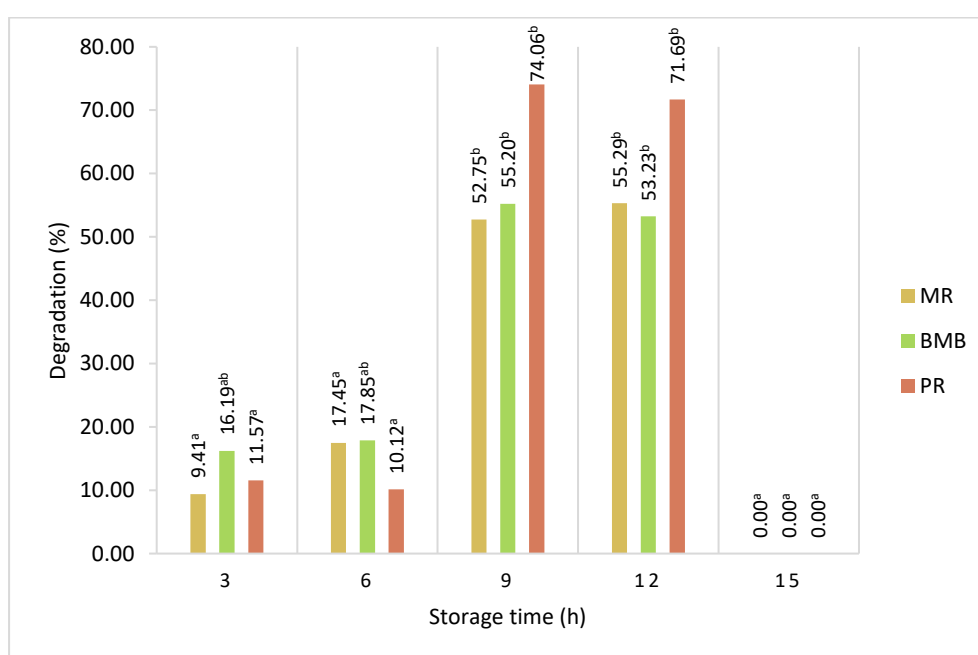

















Figure 4. Percentage of biodegradation of bacterial cellulose indicator labels (MR, BB, and PR) during 15 days of storage.

Table 2. Visual representation of the biodegradation process of bacterial cellulose indicator labels (MR, BB, and PR) during a storage period of up to 15 days.

Indicator Label	Storage Time (d)					
	0	3	6	9	12	15
MR						td
BB						td
PR						td

Note: td = totally degraded

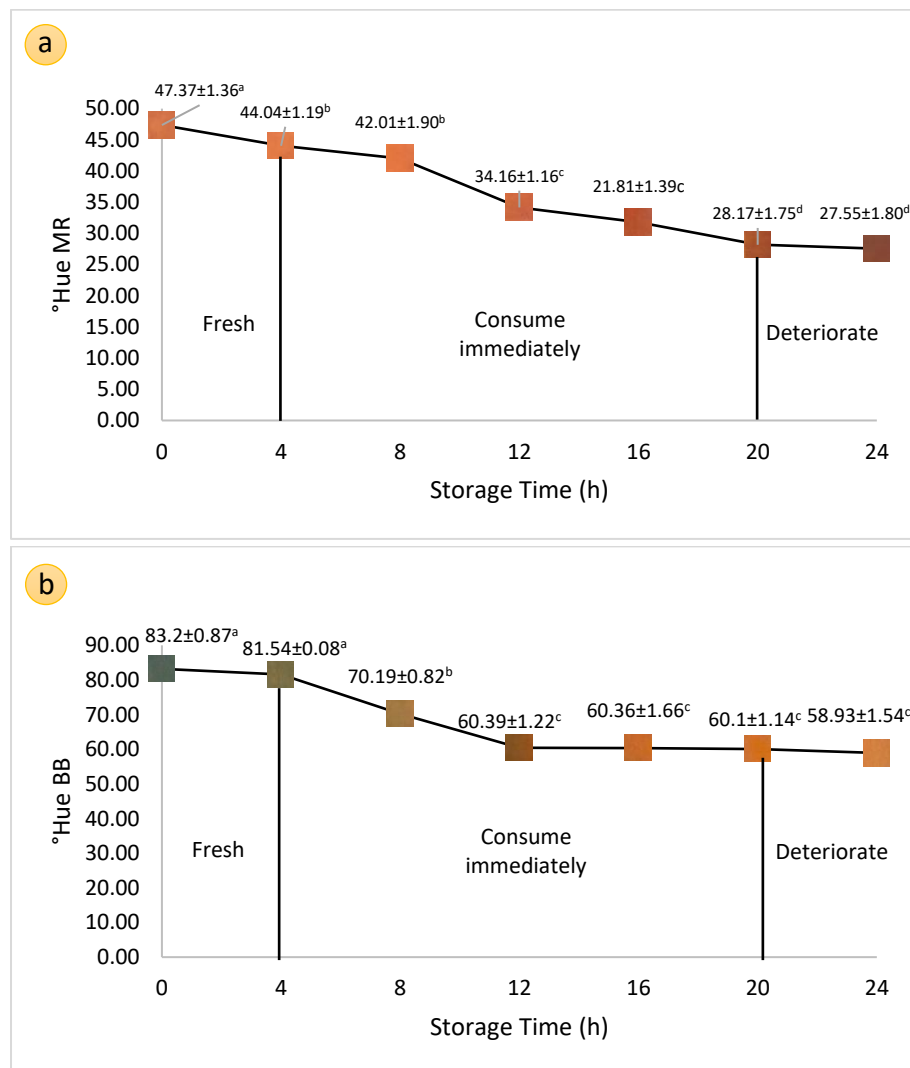
3.4. Color Properties of Bacterial Cellulose Indicator Labels and Selection of the Optimal Indicator

Colorimetric testing of the indicator labels was performed using two color parameters, namely hue angle ($^{\circ}\text{Hue}$) and delta E (ΔE). The color changes of the indicator labels resulted from the pH sensitivity of the indicators incorporated into the labels, namely methyl red, bromothymol blue, and phenol red (57). These indicators undergo color transitions in response to changes in carbon dioxide concentration inside the packaging, which serves as an indicator of fruit freshness (58). ΔE is a metric used in colorimetric testing to quantify the difference between two colors. It reflects the perceptual difference between a target color and a predicted color. The ΔE value is calculated based on differences in a multidimensional color space, where higher ΔE values indicate greater color differences (59).

Based on the results, the color changes of the indicator labels were influenced by fruit respiration activity, which increased the acidity of the storage environment and triggered shifts in indicator color. Figure 5, the methyl red and bromothymol blue labels showed a decrease in $^{\circ}\text{Hue}$ values, whereas the phenol red label exhibited an increase in $^{\circ}\text{Hue}$. The strongest test for determining the consumption limit was the Total Plate Count (TPC), as it is the most commonly used parameter to assess food safety, with microbial results indicating that the consumption limit of fresh-cut jackfruit was at 20 hours.

The methyl red indicator label displayed four phases of color change: yellow at 0 hours ($^{\circ}\text{Hue}$ 47.37), orange at 4–8 hours ($^{\circ}\text{Hue}$ 44.04–42.01), dark orange at 12–16 hours ($^{\circ}\text{Hue}$ 34.16–21.81), and reddish-orange at 20–24 hours ($^{\circ}\text{Hue}$ 28.17–27.55). This indicates that methyl red detected spoilage of fresh-cut jackfruit at 20 hours, marked by a reddish-orange label. Bromothymol blue showed three phases: green at 0 hours ($^{\circ}\text{Hue}$ 83.2), yellowish-green at 4–8 hours ($^{\circ}\text{Hue}$ 81.54–70.19), and yellowish-orange at 12–24 hours ($^{\circ}\text{Hue}$ 60.39–58.93). This suggests that bromothymol blue detected spoilage at 20 hours, indicated by a yellowish-orange label. Phenol red exhibited distinct phases: purplish-red at 0–4 hours ($^{\circ}\text{Hue}$ 15.78–24.24), red at 8–12 hours ($^{\circ}\text{Hue}$ 28.46–62.21), orange at 16–20 hours ($^{\circ}\text{Hue}$ 62.21–63.23), and yellow at 24 hours ($^{\circ}\text{Hue}$ 67.08). Based on microbial thresholds, phenol red detected spoilage at 20 hours, marked by an orange label.

Color changes in the indicator labels applied to fruit packaging were driven by jackfruit respiration as a climacteric fruit, with temperature, oxygen, and ethylene as key factors accelerating the process (60). These changes were also influenced by pH shifts in the package atmosphere, which were absorbed by the indicators (61). Similar multi-phase color changes using the three indicators have previously been reported in coconut water applications(62). Specifically, methyl red shifts from yellow under alkaline conditions (pH 6.2) to red under acidic conditions (pH 4.2); bromothymol blue shifts from green (pH 7.6) to yellow (pH 6.0); and phenol red shifts from red (pH 8.2) to yellow (pH 6.8) (63). These color transitions reflect the decline in pH within the storage atmosphere as a response to increased ethylene biosynthesis and respiration rate during fruit ripening (64).



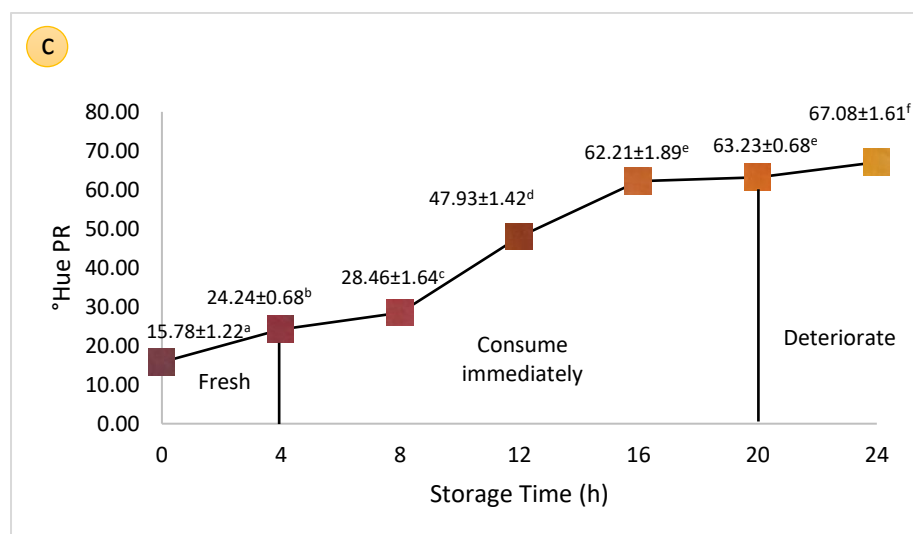


Figure 5. Color changes of bacterial cellulose indicator labels (MR, BB, PR) in fresh-cut jackfruit packaging during 24 hours at room temperature.

The ΔE value represents the magnitude of changes occurring in the color components L, a, and b*. When ΔE increases, the perceived color difference becomes more pronounced, whereas a low ΔE value indicates relatively minor or imperceptible changes (65). The evaluation scale consists of five levels: a value of 1.0 is invisible to the human eye; values of 1–2 are perceptible only upon close inspection; values of 2–10 are clearly visible at a glance; values of 11–49 indicate colors that remain similar to the original but are easily distinguishable; and a value of 100 represents two completely opposite colors (9).

Figure 6 illustrates the changes in color intensity (ΔE) of three types of indicator labels—methyl red, bromothymol blue, and phenol red—used to monitor the freshness of fresh-cut jackfruit. According to the ΔE evaluation scale, values within the range of 11–49 suggest that the colors remain relatively similar but are still easily distinguishable. During the first 4–12 hours, all three labels exhibited relatively stable color changes with no significant differences, indicating that the fruit remained fresh. A sharp increase in ΔE was observed at 16 hours, when all labels showed intense color changes: MR (48.94), BB (53.05), and PR (50.43). Between 20 and 24 hours, ΔE values remained high for all labels. In addition, Figure 7 shows how changes in the color of the indicator label on fresh jackfruit during 24 hours of storage correlate with the ΔE value obtained.

Overall, phenol red was identified as the most effective indicator, as it displayed a distinct hue shift in response to pH changes within the packaging. Although bromothymol blue exhibited the highest ΔE value, phenol red also showed high values that effectively reflected color changes in the indicator label. The strong combination of hue and ΔE responses makes phenol red the most reliable indicator for monitoring the freshness of fresh-cut jackfruit during storage.

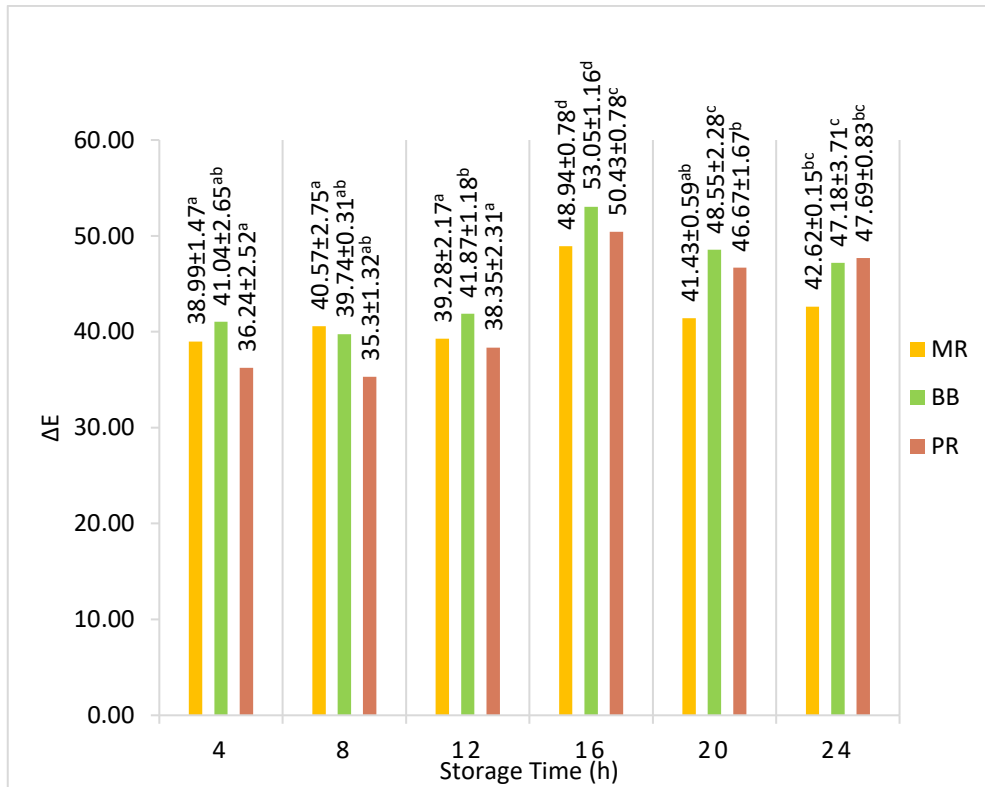


Figure 6. Delta E values of color changes in bacterial cellulose indicator labels within fresh-cut jackfruit packaging during 24 h at room temperature.

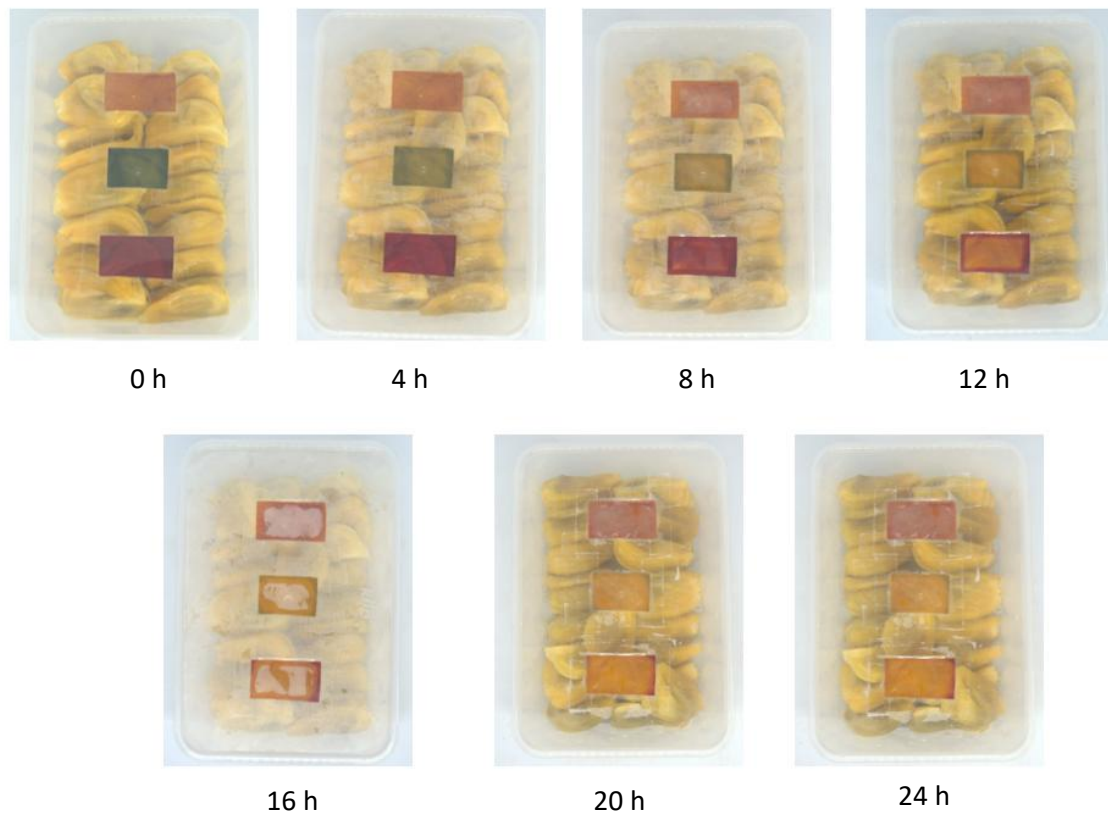


Figure 7. Visualization of bacterial cellulose indicator labels: methyl red (top), bromothymol blue (middle), and phenol red (bottom) in fresh-cut jackfruit during 24 h storage at room temperature.

3.5. Chemical Analyses of Fresh-Cut Jackfruit

Table 3 shows an increase in ΔE values of fresh-cut jackfruit during 24 hours of storage, indicating that color changes became more pronounced over time according to the ΔE evaluation scale. At 4 and 8 hours, ΔE values were within the range of 2–10 (4.39 and 8.44), meaning that color differences were visible at a glance but not yet striking. Between 12 and 24 hours (11.52–20.41), ΔE values rose to the range of 11–20, suggesting that the colors remained similar to the initial condition, but the differences were easily distinguishable to the human eye. Overall, the data confirm that noticeable color changes began after 12 hours and continued to intensify until the end of storage. This phenomenon is likely due to enzymatic browning, which becomes more evident as storage time increases. Enzymatic browning in fresh-cut fruit results from a series of biochemical and physiological processes triggered after tissue damage. It occurs when phenolic compounds stored in the vacuole are released following cell membrane disruption, commonly caused by aging or external stress that stimulates the formation of reactive oxygen species (ROS). Once released, these phenolics interact with browning enzymes such as polyphenol oxidase (PPO) and polyphenol peroxidase (POD), leading to the formation of brown pigments (66).

Changes in carbon dioxide (CO_2) and oxygen (O_2) concentrations during storage are important parameters for evaluating the physiological responses of fresh-cut fruit after slicing. During storage, respiration consumes the available oxygen inside the packaging and produces carbon dioxide and water vapor as the end products of metabolism. This respiratory activity continues until a gas equilibrium is reached within the packaging atmosphere. In fresh-cut jackfruit stored for 24 hours, CO_2 concentration gradually increased from the beginning to the end of storage. This increase indicates that respiration was actively occurring, as CO_2 is the primary product of organic compound breakdown within the tissue. Conversely, the O_2 concentration decreased over time, reflecting the typical respiration pattern of fresh-cut produce. Respiration in agricultural products is a continuous process in which oxygen (O_2) is utilized to break down complex molecules such as carbohydrates into simpler molecules, namely carbon dioxide (CO_2), water vapor (H_2O), and energy (67).

Fruit firmness is influenced by respiratory activity during storage. High firmness indicates that the fruit tissue structure remains strong, whereas a decrease in firmness reflects textural degradation caused by enzymatic activity and softening processes occurring during storage (68). Firmness testing revealed consistent reductions over 24 hours of storage, from 5.31 N at 0 hours to 2.97 N at 24 hours. Overall, this indicates that storage duration significantly affects firmness decline, reflecting the progressive softening of tissue structure during storage, as jackfruit belongs to the climacteric fruit group. Climacteric fruits continue to undergo respiration and transpiration during storage, which directly impacts firmness changes. During respiration, carbohydrate components are broken down into simpler molecules, ultimately contributing to firmness reduction and increased fruit softening (69).

A consistent decline in pH was observed during 24 hours of storage, indicating progressive acidification over time. The pH value decreased gradually from 5.20 at 0 hours to 4.48 after 24 hours of storage. This trend is attributed to the fact that jackfruit, as a climacteric fruit, is strongly influenced by physiological and biochemical dynamics occurring during ripening. One of the major changes is the reduction in pH, which is associated with enzymatic activity, depletion of organic acid reserves, and increased respiratory activity as storage progresses (61). During the climacteric phase, respiration rate and ethylene production rise sharply, promoting the utilization of organic acids such as citric and malic acid as respiratory

substrates (70). The breakdown of these organic acids releases protons, contributing to the decline in pH. In addition, enzymatic activity—such as malate enzyme—accelerates the degradation of malic acid during ripening (71), producing simpler compounds and further reducing acidity (72).

The total soluble solids (TSS) of jackfruit increased during 24 hours of storage. The initial TSS value at 0 hours was 7.83 °Brix, which remained stable at 4 hours, then began to rise at 8 hours (8.03 °Brix) and continued to increase until reaching 10.13 °Brix at 24 hours. The increase in °Brix during storage is primarily attributed to a series of biochemical processes, particularly starch hydrolysis. Starch is the major polysaccharide in jackfruit, and its breakdown into simple sugars represents a critical stage during ripening and storage. This process is catalyzed by enzymes such as α -amylase, which converts starch into glucose and fructose (73). Several studies have shown that α -amylase activity increases during storage, thereby accelerating starch conversion into soluble sugars and contributing to the rise in °Brix (74). In addition to α -amylase, other enzymes involved in carbohydrate metabolism also exhibit enhanced activity during storage, leading to a gradual accumulation of soluble sugars (75). This process occurs concurrently with climacteric respiration, a phase characterized by sharp increases in metabolic activity, including respiration and ethylene production. Elevated respiration not only accelerates starch breakdown into sugars but also influences the synthesis and activity of enzymes such as α -amylase (76). During this phase, organic acids also begin to degrade, resulting in a sweeter taste as acidity decreases and sugar concentration rises (77).

Vitamin C content in fresh-cut jackfruit was 0.013 at 0 hours of storage. The value increased at 4 hours (0.022) and reached its peak at 8 hours (0.024). After this peak, vitamin C levels gradually declined, returning close to the initial value at 24 hours (0.013). At the beginning of storage, vitamin C levels in climacteric fruits such as jackfruit tend to rise due to enhanced metabolic activity during ripening, including accelerated synthesis of ascorbic acid occurring alongside starch breakdown into simple sugars, supported by the availability of biosynthetic precursors and respiratory energy (78). Over time, however, vitamin C levels decreased as a result of enzymatic oxidation, primarily by ascorbate oxidase, which converts ascorbic acid into dehydroascorbic acid (79). This oxidative process is further accelerated when fruit is exposed to oxygen or light (80). The pattern is reinforced by climacteric respiration, in which increased respiration rate and ethylene production stimulate vitamin C synthesis but simultaneously accelerate oxidative reactions that lead to its degradation (81). At the stage approaching senescence, degradation processes become more dominant than synthesis, resulting in a net decline in vitamin C content (82).

The total acidity of jackfruit remained relatively stable at 0 and 4 hours of storage (0.09%), but increased gradually from 8 hours (0.10%) to 24 hours (0.13%). Cutting the jackfruit causes mechanical damage to fruit tissues, opening cellular compartments and releasing internal components. This injury triggers physiological responses, including the release of organic acids from damaged cells, which contributes to the rise in total acidity (83). In addition, activation of defense mechanisms due to cutting stress may stimulate the production of additional organic acids during the early stages of storage (84). After cutting, metabolic activity also intensifies. More active respiration metabolizes carbohydrates and produces organic acids such as citrate and malate, which play a central role in metabolic pathways (85). The initial accumulation of these acids leads to increased total acidity, and

certain metabolic pathways may become more dominant during storage, further promoting the production of organic acids from carbohydrate reserves(86).

The development of microbial counts (TPC, Log CFU/g) in fresh-cut jackfruit during 24 hours of storage exhibited a clear growth trend. At the beginning of storage (0 and 4 hours), microbial counts were relatively low at 3.53 and 4.05 Log CFU/g. After 8 hours, however, the counts increased sharply to approximately 5.37 Log CFU/g, indicating that microorganisms had begun to adapt and entered the active growth phase. Between 12 and 20 hours, the graph showed a consistent rise, reaching 6.64 and 7.06 Log CFU/g, which reflects the exponential phase of rapid microbial proliferation. At 24 hours, microbial counts reached 7.79 Log CFU/g, demonstrating continued growth and a decline in the microbiological quality of the fruit. The findings suggest that fresh-cut jackfruit remains acceptable for consumption up to 20 hours of storage, at which point microbial counts are still within the permissible limit of 7.7 Log CFU/g (87). The increase in microbial load is attributed to minimal processing, which accelerates microbial proliferation in fresh-cut produce. Cutting transfers surface microflora into the fruit flesh, providing a nutrient-rich medium for microbial growth (88). The presence of nutrients such as water, sugars, and organic acids in fruit tissues creates a favorable environment for microbial development, serving as substrates for microbial metabolism and facilitating the rapid increase of microbial colonies after cutting (89).

Table 3. Chemical and microbiological parameters of fresh-cut jackfruit during 24 h of storage at room temperature

Parameters	Storage Time (h)						
	0	4	8	12	16	20	24
Colorimeter (ΔE)	-	4.39±0.85 ^a	8.44±3.32 ^b	11.52±1.48 ^b	15.82±1.77 ^c	18.24±3.3 ^{cd}	20.41±2.05 ^d
O ₂ (%)	20.01±0.88 ^a	13.9±0.44 ^a	12.08±0.53 ^b	11.25±0.91 ^b	9.78±0.33 ^c	8.33±0.57 ^d	6.93±0.88 ^e
CO ₂ (%)	2.89±2.55 ^a	8.81±2.79 ^b	11.04±0.71 ^b	14.03±1.5 ^c	18.15±0.47 ^d	21.93±1.46 ^e	24.95±2.57 ^e
Firmness (N)	5.13±0.45 ^a	4.77±0.35 ^{ab}	4.33±0.4 ^{bc}	3.97±0.64 ^{cd}	3.9±0.62 ^{cd}	3.2±0 ^{de}	2.97±0.12 ^e
pH	5.2±0.09 ^a	5.07±0.32 ^{ab}	4.88±0.16 ^{abc}	4.75±0.23 ^{abc}	4.73±0.21 ^{abc}	4.6±0.1 ^{bc}	4.48±0.62 ^c
TSS (°Brix)	7.83±0.59	7.83±0.75	8.03±0.55	8.6±1.51	9.17±2.08	9.5±2.77	10.13±2.83
Vitamin C	0.013±0.002	0.022±0.013	0.023±0.012	0.022±0.012	0.019±0.004	0.017±0.005	0.013±0.001
Total Acidity (%)	0.09±0.01	0.09±0.01	0.1±0.01	0.11±0.01	0.12±0.013	0.13±0.013	0.13±0.06
TPC (Log CFU/g)	3.53±0.37 ^a	4.050.87 ^a	5.37±0.1 ^b	6.64±0.05 ^c	6.92±0.01 ^c	7.06±0.03 ^c	7.79±0.04 ^d

Note: TSS= Total Soluble Solids. Values are expressed as mean ± standard deviation. Different superscript letters within the same row indicate statistically significant differences (p < 0.05)

3.6. Indicator Label Response in Relation to Quality Degradation of Fresh-Cut Jackfruit During Storage

Correlation analysis was conducted to obtain a comprehensive overview of the response of the selected indicator label (PR) to quality changes in fresh-cut jackfruit during storage. The parameters included O₂ and CO₂ concentrations, firmness, pH, total soluble solids, vitamin C, total acidity, and Total Plate Count (TPC), which was analyzed to assess

microbial growth dynamics. Figure 7 presents the changes in all these parameters throughout the storage period, enabling evaluation of the relationships among variables and how each contributes to the overall decline in fruit quality.

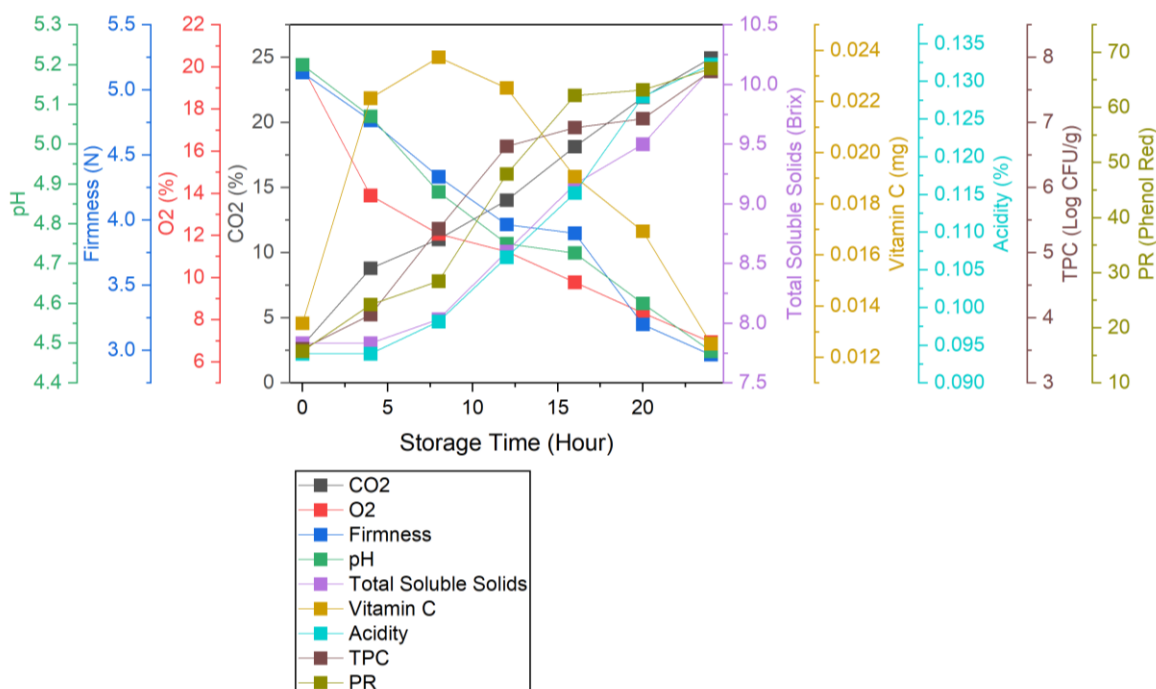


Figure 7. Correlation level between indicator label response and various quality deterioration parameters of fresh-cut jackfruit during storage.

Based on Figure 7, the quality parameters of fresh-cut jackfruit during 24 h of storage are illustrated. The changes in various parameters are interrelated and reflect a series of physiological, chemical, and microbiological processes occurring during storage. The increase in CO₂ accompanied by the decrease in O₂ indicates that fruit respiration remained active after cutting (67), and this respiratory activity subsequently triggered tissue softening, leading to reduced firmness (68). Respiration and the breakdown of internal components also contributed to the decline in pH (71). At the same time, changes in total soluble solids reflected carbohydrate degradation that supported metabolic activity (74).

The reduction in vitamin C was attributed to oxidation accelerated by storage conditions and increased metabolic activity (81). The rise in total acidity resulted from tissue injury that stimulated the release of organic acids from damaged cells (83). Meanwhile, microbial growth, as indicated by the increase in TPC, occurred in parallel with decreasing pH and rising total acidity, since more acidic conditions and higher levels of soluble substrates provided a favorable environment for certain microorganisms. Finally, the color change of phenol red reflected the chemical composition shifts in the fruit during storage.

4. Conclusions

The study confirmed that bacterial cellulose-based indicator labels integrated with colorimetric solutions can serve as an effective tool for intelligent packaging of fresh-cut jackfruit. By identifying the most appropriate color indicator and validating its performance, the research demonstrated that the developed label responds consistently to physiological,

chemical, and microbiological changes during storage. The correlation between color shifts and quality parameters highlights the reliability of this system in detecting freshness levels. These outcomes emphasize the potential of bacterial cellulose indicator labels to provide a simple, real-time visual signal of fruit quality, supporting both consumer confidence and industrial applications in maintaining product safety.

Acknowledgements

The authors would like to express thanks to The Indonesian Ministry of Higher Education, Science, and Technology (KEMDIKTISAINTEK) for providing funding which made this work possible.

Author Contributions

N.I. writing original draft, conceptualization, and validation; A.D. writing original draft, investigation, methodology, and supervision; A.S. writing original draft, data curation; S.H.H. writing – review & editing; A.F.A. vizualization and writing – review & editing; S.M. Writing – review & editing

Funding

This project was funded by The Indonesian Ministry of Higher Education, Science, and Technology (KEMDIKTISAINTEK), Penelitian Tesis Magister, under grant no. (PTM), 124/E5/PG.02.00.PL/2023.

Institutional Review Board Statement

Not applicable.

Data Availability Statement

Available data are presented in the manuscript.

Conflicts of Interest

The authors declared no conflict of interest.

References

1. Heerschop SN, Biesbroek S, Temme EHM, Ocké MC. Can healthy and sustainable dietary patterns that fit within current dutch food habits be identified? *Nutrients*. 2021;13(4).
2. He X, Pu Y, Chen L, Jiang H, Xu Y, Cao J, et al. A comprehensive review of intelligent packaging for fruits and vegetables: Target responders, classification, applications, and future challenges. *Compr Rev Food Sci Food Saf*. 2023 Mar;22(2):842–81.
3. Holte T, Id S, Nordheim O, Bere E, Eikemo TA. Fruit and vegetable consumption in Europe according to gender, educational attainment and regional affiliation-A cross-sectional study in 21 European countries. 2020;
4. Macieira A, Barbosa J, Teixeira P. Food safety in local farming of fruits and vegetables. *Int J Environ Res Public Health*. 2021;18(18).
5. Hermansyah D, Patiung M, Wisnujati NS. Analisis Trend dan Prediksi Produksi dan Konsumsi Komoditas Sayuran Sawi (*Brassica Juncea L*) di Indonesia Tahun 2020 s/d

2029. J Ilm Sosio Agribis. 2021 Dec;21(2).
6. Santin F, Gabe KT, Levy RB, Jaime PC. Food consumption markers and associated factors in Brazil: distribution and evolution, *Brazilian National Health Survey*, 2013 and 2019. *Cad Saude Publica*. 2022;38:e00118821.
 7. Ameri M, Aji A, Kessler S. Enhancing Seafood Freshness Monitoring: Integrating Color Change of a Food-Safe On-Package Colorimetric Sensor with Mathematical Models, Microbiological, and Chemical Analyses. 2024 Oct;
 8. Mohammed M, Srinivasagan R, Alzahrani A, Alqahtani NK. Machine-Learning-Based Spectroscopic Technique for Non-Destructive Estimation of Shelf Life and Quality of Fresh Fruits Packaged under Modified Atmospheres. *Sustain*. 2023;15(17).
 9. Dirpan A, Djalal M, Ainani AF. A Simple Combination of Active and Intelligent Packaging Based on Garlic Extract and Indicator Solution in Extending and Monitoring the Meat Quality Stored at Cold Temperature. *Foods*. 2022;11(10):1495.
 10. Luo X, Zaitoon A, Lim LT. A review on colorimetric indicators for monitoring product freshness in intelligent food packaging: Indicator dyes, preparation methods, and applications. *Compr Rev Food Sci Food Saf*. 2022 May;21(3):2489–519.
 11. Panou A, Lazaridis DG, Karabagias IK, Panou A, Lazaridis DG, Karabagias IK. Application of Smart Packaging on the Preservation of Different Types of Perishable Fruits. *Foods* 2025, Vol 14,. 2025 May;14(11).
 12. Liu D, Zhang C, Pu Y, Chen S, Liu L, Cui Z, et al. Recent Advances in pH-Responsive Freshness Indicators Using Natural Food Colorants to Monitor Food Freshness. *Foods*. 2022;11(13).
 13. Yu Z, Boyarkina V, Liao Z, Lin M, Zeng W, Lu X. Boosting Food System Sustainability through Intelligent Packaging: Application of Biodegradable Freshness Indicators. *ACS Food Sci Technol*. 2023 Jan;3(1):199–212.
 14. Alam AU, Rath P, Beshai H, Sarabha GK, Deen MJ, Alam AU, et al. Fruit Quality Monitoring with Smart Packaging. *Sensors* 2021, Vol 21,. 2021 Feb;21(4):1–30.
 15. Zhai X, Xue Y, Sun Y, Ma X, Ban W, Marappan G, et al. Colorimetric Food Freshness Indicators for Intelligent Packaging: Progress, Shortcomings, and Promising Solutions. *Foods*. 2025;14(16):1–34.
 16. Kamaruddin I, Dirpan A, Bastian F. The novel trend of bacterial cellulose as biodegradable and oxygen scavenging films for food packaging application : An integrative review. In: *IOP Conference Series: Earth and Environmental Science*. 2021.
 17. Abdelkader RMM, Hamed DA, Gomaa OM. Red cabbage extract immobilized in bacterial cellulose film as an eco-friendly sensor to monitor microbial contamination and gamma irradiation of stored cucumbers. *World J Microbiol Biotechnol* 2024 409. 2024 Jul;40(9):258-.
 18. Dikshit PK. Production of Low-Cost Nano-Functionalized Bacterial Cellulose Films for Smart/Intelligent Packaging. 2023;58.
 19. Dirpan A, Djalal M, Kamaruddin I, Dirpan A, Djalal M, Kamaruddin I. Application of an Intelligent Sensor and Active Packaging System Based on the Bacterial Cellulose of *Acetobacter xylinum* to Meat Products. *Sensors* 2022, Vol 22,. 2022 Jan;22(2).
 20. Li N, Yang X, Lin D. Development of bacterial cellulose nanofibers/konjac glucomannan-based intelligent films loaded with curcumin for the fresh-keeping and freshness monitoring of fresh beef. *Food Packag Shelf Life*. 2022;34(May):100989.
 21. Rasouli Y, Moradi M, Tajik H, Molaei R. Fabrication of anti-*Listeria* film based on

- bacterial cellulose and *Lactobacillus sakei*-derived bioactive metabolites; application in meat packaging. *Food Biosci.* 2021;42(April):101218.
22. Zhou S, Li N, Peng H, Yang X, Lin D. The Development of Highly pH-Sensitive Bacterial Cellulose Nanofibers/Gelatin-Based Intelligent Films Loaded with Anthocyanin/Curcumin for the Fresh-Keeping and Freshness Detection of Fresh Pork. *Foods.* 2023;12(20).
 23. Ahmed M, Bose I, Nousheen, Roy S. Development of Intelligent Indicators Based on Cellulose and *Prunus domestica* Extracted Anthocyanins for Monitoring the Freshness of Packaged Chicken. *Int J Biomater.* 2024;2024.
 24. Tohamy HAS. A novel anthocyanins hydroxyethyl cellulose film for intelligent chicken meat packaging with mechanical study, DFT calculations and molecular docking study. *Sci Rep.* 2025;15(1):1–15.
 25. Pirsá S, Shamusí T. Intelligent and active packaging of chicken thigh meat by conducting nano structure cellulose-polypyrrole-ZnO film. *Mater Sci Eng C.* 2019;102(February):798–809.
 26. Ardiani S, Dany Rahmayanti H, Setiadi D, Ginting JC, Akmalia N, Kartika TR, et al. Application of Anthocyanin Extracted from Purple Sweet Potato and Nata de Coco Film in The Smart Food Packaging Technology. *J Tekno.* 2023 Jun;20(1):15–23.
 27. Ludwicka K, Kaczmarek M, Białkowska A, Ludwicka K, Kaczmarek M, Białkowska A. Bacterial Nanocellulose—A Biobased Polymer for Active and Intelligent Food Packaging Applications: Recent Advances and Developments. *Polym* 2020, Vol 12,. 2020 Sep;12(10):1–23.
 28. Zhou X, Liu X, Liao W, Wang Q, Xia W. Chitosan/bacterial cellulose films incorporated with tea polyphenol nanoliposomes for silver carp preservation. *Carbohydr Polym.* 2022;297(September):120048.
 29. Mohseni-Shahri F, Mehrzad A, Khoshbin Z, Sarabi-Jamab M, Khanmohamadi F, Verdian A. Polyphenol-loaded bacterial cellulose nanofiber as a green indicator for fish spoilage. *Int J Biol Macromol.* 2023 Jan;224:1174–82.
 30. Liu H, Shi C, Sun X, Zhang J, Ji Z. Intelligent colorimetric indicator film based on bacterial cellulose and pelargonidin dye to indicate the freshness of tilapia fillets. *Food Packag Shelf Life.* 2021 Sep;29:100712.
 31. Atta OM, Manan S, Ul-Islam M, Ahmed AAQ, Ullah MW, Yang G. Development and characterization of plant oil-incorporated carboxymethyl cellulose/bacterial cellulose/glycerol-based antimicrobial edible films for food packaging applications. *Adv Compos Hybrid Mater* 2022 52. 2022 Jan;5(2):973–90.
 32. Melnyk H, Havryliuk O, Zaets I, Sergeyeva T, Zubova G, Korovina V, et al. Red Cabbage Anthocyanin-Loaded Bacterial Cellulose Hydrogel for Colorimetric Detection of Microbial Contamination and Skin Healing Applications. *Polymers (Basel).* 2025;17(15):1–18.
 33. Liu X, Xu Y, Liao W, Guo C, Gan M, Wang Q. Preparation and characterization of chitosan/bacterial cellulose composite biodegradable films combined with curcumin and its application on preservation of strawberries. *Food Packag Shelf Life.* 2023 Mar;35:101006.
 34. Ran R, Wang L, Su Y, He S, He B, Li C, et al. Preparation of pH-indicator films based on soy protein isolate/bromothymol blue and methyl red for monitoring fresh-cut apple freshness. *J Food Sci.* 2021 Oct;86(10):4594–610.

35. Dodange S, Shekarchizadeh H, Kadivar M. Real-time tracking of fish quality using a cellulose filter paper colorimetric indicator incorporated with prickly pear fruit betacyanins. *Lwt.* 2024;205(July):116523.
36. A.F. HSH. DA. ADM. RANF. A. Sensitivity determination of indicator paper as smart packaging elements in monitoring meat freshness in cold temperature. *IOP Conf Ser Earth Environ Sci.* 2019;343.
37. Herawati H, Kamsiati E, Widyaputri S, Sutanto. Physic-chemical characteristic of nata de coco. *IOP Conf Ser Earth Environ Sci.* 2020;458(1).
38. Bodea IM, Beteg FI, Pop CR, David AP, Dudescu MC, Vilău C, et al. Optimization of moist and oven-dried bacterial cellulose production for functional properties. *Polymers (Basel).* 2021 Jul;13(13):2088.
39. Gea S, Reynolds CT, Roohpour N, Wirjosentono B, Soykeabkaew N, Bilotti E, et al. Investigation into the structural, morphological, mechanical and thermal behaviour of bacterial cellulose after a two-step purification process. *Bioresour Technol.* 2011 Oct;102(19):9105–10.
40. Suryanto H. Analisis Struktur Serat Selulosa Dari Bakteri. *Pros SNTT* 2017. 2017;3(October):17–22.
41. Amorim LFA, Fangueiro R, Gouveia IC. Characterization of Bioactive Colored Materials Produced from Bacterial Cellulose and Bacterial Pigments. *Mater* 2022, Vol 15, Page 2069. 2022 Mar;15(6):2069.
42. Pinandoyo MU, Hastuti S. Journal of Aquaculture Management and Technology Online di : <http://ejournal-s1.undip.ac.id/index.php/jamt> Journal of Aquaculture Management and Technology. *J Aquac Manag Technol.* 2017;6:169–78.
43. Fitriyah H, Wihandika RC. An Analysis of RGB, Hue and Grayscale under Various Illuminations. 3rd Int Conf Sustain Inf Eng Technol SIET 2018 - Proc. 2018 Jul;38–41.
44. Pasieczna-Patkowska S, Cichy M, Flieger J. Application of Fourier Transform Infrared (FTIR) Spectroscopy in Characterization of Green Synthesized Nanoparticles. Vol. 30, *Molecules.* 2025.
45. Mochochoko T, Oluwafemi OS, Jumbam DN, Songca SP. Green synthesis of silver nanoparticles using cellulose extracted from an aquatic weed; Water hyacinth. *Carbohydr Polym.* 2013;98(1):290–4.
46. Sivanantham G, Sivaraj Vijaya G, Murugan A, Selvaraj S, Thangavelu K, Mani SK, et al. Characterization and physicochemical properties of lignocellulosic fibers from Fishtail Palm (*Caryota mitis*) Leaf Stalks . *Compos Adv Mater.* 2024 Feb;33:1–12.
47. Gopinath R, Billigraham P, Sathishkumar TP. Physico-Chemical, Mechanical and Thermal Properties of Novel Cellulosic Fiber Extracted from the Bark of *Tithonia Diversifolia*. *J Nat Fibers.* 2023;20(1).
48. Gayathry G, Gopalaswamy G. Production and characterisation of microbial cellulosic fibre from *Acetobacter xylinum*. *Indian J Fibre Text Res.* 2014;39(1):93–6.
49. Zhang PP, Tong DS, Lin CX, Yang HM, Zhong ZK, Yu WH, et al. Effects of acid treatments on bamboo cellulose nanocrystals. *Technology.* 2009 Sep;7(17):743–53.
50. Nurjannah NR, Sudiarti T, Rahmidar L. Sintesis dan Karakterisasi Selulosa Termetilasi sebagai Biokomposit Hidrogel. *al-Kimiya.* 2020;7(1):19–27.
51. Rahmayetty B, Toha M, Kanani N. Proceedings of the 2nd International Conference for Smart Agriculture, Food, and Environment (ICSAFE 2021). Vol. 1, Proceedings of the 2nd International Conference for Smart Agriculture, Food, and Environment (ICSAFE

- 2021). Atlantis Press International BV; 2023. 99–106 p.
52. Saravanakumar SS, Kumaravel A, Nagarajan T, Sudhakar P, Baskaran R. Characterization of a novel natural cellulosic fiber from Prosopis juliflora bark. *Carbohydr Polym.* 2013 Feb;92(2):1928–33.
 53. Senthamaraikannan P, Sanjay MR, Bhat KS, Padmaraj NH, Jawaaid M. Characterization of natural cellulosic fiber from bark of Albizia amara. *J Nat Fibers.* 2019;16(8):1124–31.
 54. Demirbas A. Biodegradable plastics from renewable resources. *Energy Sources, Part A Recover Util Environ Eff.* 2007;29(5):419–24.
 55. Srikandace Y, Andayani DGS, Karina M. Preliminary study of the degradation of biocellulose based film using soil fungi *Aspergillus unguis* TP3 and *Paecilomyces marquandii* TP4 producing cellulose. *IOP Conf Ser Earth Environ Sci.* 2019;277(1).
 56. Zahan KA, Azizul NM, Mustapha M, Tong WY, Rahman MSA, Sahuri IS. Application of bacterial cellulose film as a biodegradable and antimicrobial packaging material. *Mater Today Proc.* 2020;31(xxxx):83–8.
 57. Rong L, Zhang T, Ma Y, Wang T, Liu Y, Wu Z. An intelligent label using sodium carboxymethyl cellulose and carrageenan for monitoring the freshness of fresh-cut papaya. *Food Control.* 2023 Mar;145.
 58. Pablo AG, Galvez L, Lauzon R, Diczbalis Y. Physicochemical qualities of stored fresh cut EVIARC sweet jackfruit (*Artocarpus heterophyllus* Lam.) pulp as influenced by deseeding, packaging method and storage condition. *Ann Trop Res.* 2019 May;138–54.
 59. Willis RF, X-Rite I. DELTA E FORMULA MATCH PREDICTION. X-Rite, Incorporated; 2022.
 60. Ye S, Anil R, Kulkarni P, Nawaz A, Imran A, Yadav D, et al. Enhancing Jackfruit Shelf-Life Through Intelligent Packaging: A Review. *Food Rev Int.* 2025;00(00):1–27.
 61. Mujahidah A, Sukainah A, Indrayani. Pemanfaatan Molase Sebagai Substrat. 2020;9:193–202.
 62. Dirpan A, Langkong J, Laga A, Djalal M, Khosuma M, Nurhisna NI, et al. Fabrication of freshness indicators based on methylcellulose-containing color indicator solutions for monitoring the quality of coconut water. *Heliyon [Internet].* 2024 Mar 30;10(6). Available from: <https://doi.org/10.1016/j.heliyon.2024.e28317>
 63. Ka S, Ki A, Ok R. pH Indicators: A Valuable Gift for Analytical Chemistry. *Saudi J Med Pharm Sci Abbreviated Key Title Saudi J Med Pharm Sci ISSN.*
 64. Kaur J, Singh Z, Shah HMS, Mazhar MS, Hasan MU, Woodward A. Insights into phytonutrient profile and postharvest quality management of jackfruit: A review. *Crit Rev Food Sci Nutr.* 2024;64(19):6756–82.
 65. Baselia D, Zulaikhah S, Rejeki APS, Govi BG, Rizki R. Pengaruh Suhu Penyangaian Terhadap Sifat Fisikokimia dan Tingkat Kesukaan Kopi Robusta. *J Food Agric Technol.* 2024 Nov;2(1):1–11.
 66. Sommano SR, Chanasut U, Kumpoun W. Enzymatic browning and its amelioration in fresh-cut tropical fruits. *Fresh-Cut Fruits Veg Technol Mech Saf Control.* 2020 Jan;51–76.
 67. Nugraha B, Nidaa' A, Rahmah F, Ayuningsih I, Priyanti D, Affandi FY. A Comparative Study of Respiratory Activity of Tropical Products under Two Storage Conditions. *J Tek Pertan Lampung (Journal Agric Eng.* 2024 Mar;13(1):269–77.
 68. Tiolyn Rohana Sitorus R, Hartiati A, Wayan Gede Sedana Yoga I. Characteristics Of Fresh-Cut California Papaya Treated With Cassava Starch-Chitosan Ratios And Glycerol Concentrations As Edible Coating. *J REKAYASA DAN Manaj AGROINDUSTRI.* 2025

- Sep;13(3):309–20.
69. Kusumiyati K, Farida F, Sutari W, Mubarak S. Mutu buah sawo selama periode simpan berbeda. *Kultivasi*. 2017 Jan;16(3).
 70. Ding R, Dai X, Zhang Z, Bi Y, Prusky D. Composite Coating of Oleaster Gum Containing Cuminal Keeps Postharvest Quality of Cherry Tomatoes by Reducing Respiration and Potentiating Antioxidant System. 2024 Apr;
 71. Zhou X, Cheng J, Sun J, Guo S, Guo X, Chen Q, et al. Effect of Red Visible Lighting on Postharvest Ripening of Bananas via the Regulation of Energy Metabolism. *Hortic* 2023, Vol 9, Page 840. 2023 Jul;9(7):840.
 72. Jiang CC, Fang ZZ, Zhou DR, Pan SL, Ye XF. Changes in secondary metabolites, organic acids and soluble sugars during the development of plum fruit cv. 'Furongli' (*Prunus salicina* Lindl). *J Sci Food Agric*. 2019 Feb;99(3):1010–9.
 73. Patel PR, Gol NB, Ramana Rao T V. Physiochemical changes in sunberry (*Physalis minima* L.) fruit during growth and ripening. *Fruits*. 2011;66(1):37–46.
 74. Masserano G, Moretti B, Bertora C, Vidotto F, Monaco S, Vocino F, et al. Acetic acid disturbs rice germination and post-germination under controlled conditions mimicking green mulching in flooded paddy. *Ital J Agron*. 2022 Jan;17(1):1926.
 75. Hussain S, Khan F, Hussain HA, Nie L. Physiological and biochemical mechanisms of seed priming-induced chilling tolerance in rice cultivars. *Front Plant Sci*. 2016 Feb;7(FEB2016):178194.
 76. Hernández-Hernández H, Quiterio-Gutiérrez T, Cadenas-Pliego G, Ortega-Ortiz H, Hernández-Fuentes AD, De La Fuente MC, et al. Impact of Selenium and Copper Nanoparticles on Yield, Antioxidant System, and Fruit Quality of Tomato Plants. *Plants* 2019, Vol 8, Page 355. 2019 Sep;8(10):355.
 77. Bhardwaj R, Pareek S, Mani S, Domínguez-Avila JA, González-Aguilar GA. A Melatonin Treatment Delays Postharvest Senescence, Maintains Quality, Reduces Chilling Injury, and Regulates Antioxidant Metabolism in Mango Fruit. *J Food Qual*. 2022;2022.
 78. Chen C, Guo J, Kahramanoğlu İ, Wan C, Gan Z, Chen J. Biocontrol Bacterium *Paenibacillus brasiliensis* YS-1 Fermented Broth Enhances the Quality Attributes and Storability of Harvested "Newhall" Navel Oranges. *ACS Food Sci Technol*. 2020 Feb;1(1):88–95.
 79. Ali Q, Kurubas MS, Ustun H, Erkan M. Determination of nutritional values and postharvest performance in different types of tomatoes stored under shelf-life conditions. *Mediterr Agric Sci*. 2020 Apr;33(1):9–14.
 80. Ponder A, Jariéné E, Hallmann E. The Effect of Storage Conditions on the Content of Molecules in *Malus domestica* 'Chopin' cv. and Their In Vitro Antioxidant Activity. *Molecules*. 2022 Oct;27(20):6979.
 81. Zhang J, Ma Y, Dong C, Terry LA, Watkins CB, Yu Z, et al. Meta-analysis of the effects of 1-methylcyclopropene (1-MCP) treatment on climacteric fruit ripening. *Hortic Res*. 2020 Dec;7(1):208.
 82. Rehman MA, Asi MR, Hameed A, Bourquin LD. Effect of Postharvest Application of Aloe Vera Gel on Shelf Life, Activities of Anti-Oxidative Enzymes, and Quality of 'Gola' Guava Fruit. *Foods* 2020, Vol 9, Page 1361. 2020 Sep;9(10):1361.
 83. Kumari J, Nikhanj P. Evaluation of edible coatings for microbiological and physicochemical quality maintenance of fresh cut papaya. *J Food Process Preserv*. 2022 Oct;46(10):e16790.

84. Poornakala J. Enhancement of Shelf Life of Jackfruit Bulbs through Edible Coating: A Mini Review. *J Sci Res Reports*. 2023 Jun;29(7):27–31.
85. Ruiz-Martínez J, Aguirre-Joya JA, Rojas R, Vicente A, Aguilar-González MA, Rodríguez-Herrera R, et al. Candelilla Wax Edible Coating with *Flourensia cernua* Bioactives to Prolong the Quality of Tomato Fruits. *Foods* 2020, Vol 9, Page 1303. 2020 Sep;9(9):1303.
86. Marín A, Baldwin EA, Bai J, Wood D, Ference C, Sun X, et al. Edible Coatings as Carriers of Antibrowning Compounds to Maintain Appealing Appearance of Fresh-cut Mango. *Horttechnology*. 2021 Feb;31(1):27–35.
87. Bizura Hasida MR, Nur Aida MP, Zaipun MZ, Hairiyah M. Microbiological changes of minimally processed jackfruit after UV-C treatment. *Acta Hortic*. 2013;1012:1025–30.
88. Qadri OS, Yousuf B, Srivastava AK. Fresh-cut fruits and vegetables: Critical factors influencing microbiology and novel approaches to prevent microbial risks—A review. *Cogent Food Agric*. 2015 Dec;1(1):1121606.
89. Quaye AK, Badu M, Kushitor SB, Badu K. Microbial Load and Chemical Composition of Tomato (*Lycopersicon esculentum*) During Market Storage. 2025 May;